

Transient ATM Kinase Inhibition Disrupts DNA Damage–Induced Sister Chromatid Exchange

Jason S. White,^{1,2} Serah Choi,³ Christopher J. Bakkenist^{1,4*}

(Published 1 June 2010; Volume 3 Issue 124 ra44)

Cells derived from ataxia telangiectasia (A-T) patients exhibit defective cell cycle checkpoints because of mutations in the gene encoding ATM (ataxia telangiectasia mutated). After exposure to ionizing radiation (IR), A-T cells exhibit sensitivity to IR-induced cellular damage that results in increased chromosome aberrations and cell death (radiosensitivity). ATM is a member of a family of kinases that become activated in response to DNA damage. We showed that even transient inhibition of ATM kinase for 1 hour 15 min after cellular irradiation resulted in an accumulation of persistent chromosome aberrations and increased cell death. Using reversible inhibitors of DNA-PK (DNA-dependent protein kinase), another kinase involved in responding to DNA damage, and ATM, we showed that these two kinases acted through distinct DNA repair mechanisms: ATM resolved DNA damage through a mechanism involving sister chromatid exchange (SCE), whereas DNA-PK acted through nonhomologous end joining. Furthermore, because DNA damage–induced SCE occurred in A-T fibroblasts that lack functional ATM protein, and the inhibitors of ATM kinase had no effect on DNA damage–induced SCE in A-T fibroblasts, we showed that the consequences of short-term inhibition of the kinase activity of ATM and adaptation to ATM protein disruption were distinct. This suggests that A-T fibroblasts have adapted to the loss of ATM and have alternative mechanisms to initiate SCE.

INTRODUCTION

Ataxia telangiectasia (A-T) is a childhood disorder characterized by neurodegeneration, predisposition to cancers, and profound, lethal sensitivity to ionizing radiation (radiosensitivity). A-T is caused by either compound heterozygosity or homozygosity for truncating mutations (frameshift or nonsense mutations) in the *ataxia telangiectasia mutated* (*ATM*) gene, resulting in an absence of detectable ATM protein (1, 2). *ATM* encodes a protein kinase that is critical for the initiation of DNA damage responses in mammalian cells exposed to ionizing radiation (IR) or to other agents that introduce double-strand breaks (DSBs) into DNA (1, 3, 4). Cells derived from A-T patients exhibit defective cell cycle checkpoint responses, increased chromosome aberrations, and increased cell death after IR, thus revealing the importance of ATM-dependent signaling in irradiated cells (5).

ATM belongs to a family of kinases, the phosphoinositide 3-kinase–related protein kinases, that function in DNA damage responses. The kinase activity of ATM is extremely sensitive to DNA damage and is activated in cells within seconds of exposure to doses as low as 0.1 gray (Gy) IR (6). The kinase activity of ATM is essential for the activation of downstream effector kinases, such as checkpoint kinase 2 (CHK2) (7), and the phosphorylation of numerous substrates that impede origin firing (the initiation of DNA replication at a particular origin) during S phase (8) and that halt the progression of the cell cycle at the G₁-S phase (9) and G₂-M phase (10) transitions. Such cell cycle checkpoints were envisioned as transient delays of the cell cycle that allow sufficient time for chromosome repair and

that prevent cell cycle progression in the presence of chromosome damage (11). However, the chromosomal instability of A-T cells may not be entirely due to defective cell cycle checkpoints. Chromosome aberrations accumulated in irradiated A-T cells arrested in G₀ for up to 48 hours, indicating this damage is not a consequence of defective cell cycle checkpoints (12, 13). Similarly, when aphidicolin was used to block the G₁-S phase transition in A-T cells, no decrease in cell death was observed after IR (14). Because increased chromosome aberrations and cell death were evident in cells that were not progressing through the cell cycle, these data are indicative of a DNA repair defect in A-T cells that is independent of cell cycle checkpoints.

The repair of DSBs can occur through nonhomologous end joining (NHEJ) or homologous recombination (HR) and the kinase activity of ATM has been implicated in both mechanisms. HR is a high-fidelity DSB repair mechanism that is generally restricted to the S and G₂ phases of the cell cycle when a sister chromatid is available as a repair template (15). ATM promotes the HR-mediated repair of DSBs in various systems, including in DT40 chicken cells in response to IR (16) and in Chinese hamster cells in response to inhibition of poly(adenosine diphosphate ribose) polymerase (PARP) (17). Furthermore, the kinase activity of ATM participates in DSB end resection, which is a key step in HR (18). Nevertheless, sister chromatid exchange (SCE), which occurs through HR-mediated repair, is normal in A-T cells (19–21). NHEJ operates throughout the cell cycle but is particularly important in G₁ when a sister chromatid is not available as a repair template (22). The NHEJ machinery includes the DNA-dependent protein kinase (DNA-PK), a heterotrimer comprising a catalytic subunit and KU70 and KU80, a heterodimer of LIG IV and XRCC4 that has ligase activity, and the Artemis endonuclease. ATM-dependent Artemis activity is required for the resolution of ~10% of DSBs by NHEJ that are repaired within several hours after IR (23).

Although the ATM-dependent mobilization, modification, and stimulation of proteins after IR is well documented (24, 25), the mechanisms by which ATM ensures cellular radioprotection and genome stability are not fully understood. Indeed, it is particularly challenging to causally relate the changes in ATM activity to changes in the phosphorylation status of a specific substrate that may cause a particular disease or phenotype, because

¹Department of Radiation Oncology, University of Pittsburgh Medical School, Hillman Cancer Center, Research Pavilion, Suite 2.6, 5117 Centre Avenue, Pittsburgh, PA 15213–1863, USA. ²BioCytics, Inc, 9801 W Kinsey Avenue, Suite 145, Huntersville, NC 28078, USA. ³Medical Scientist Training Program, Molecular Pharmacology Graduate Program, University of Pittsburgh Medical School, Pittsburgh, PA 15213–1863, USA. ⁴Department of Pharmacology and Chemical Biology, University of Pittsburgh Medical School, Hillman Cancer Center, Pittsburgh, PA 15213–1863, USA.

*To whom correspondence should be addressed. E-mail: bakkenistcj@upmc.edu

there appears little selective pressure to restrict functionally insignificant phosphorylation events, as suggested by the >1000 ATM and ATR (ATM and Rad3-related) substrates identified (24, 25). However, better understanding of the mechanisms by which ATM contributes to radioprotection and genome stability may allow the rational design of clinical protocols that use inhibitors of ATM activity, which is particularly relevant because inhibition of the kinase activity of ATM selectively kills tumor cells with certain somatic mutations, while sparing normal cells. In the absence of treatments to induce DNA damage, inhibition of the kinase activity of ATM with KU55933 reduced long-term survival of Fanconi anemia (FA)-deficient pancreatic tumor cell lines, but not isogenic corrected control cell lines (26). This same inhibitor reduced the long-term survival of doxorubicin-treated p53-deficient lung tumor cell lines, lymphocytes, and mouse embryonic fibroblasts (MEFs), whereas KU55933 inhibition of the kinase activity of ATM in cell lines with functional p53 increased the resistance of these cells to the lethal effects of doxorubicin, a DNA-damaging agent (27, 28). Thus, pharmacological inhibition of the kinase activity of ATM may have a role in the treatment of both FA-deficient and p53-deficient human cancers.

KU55933 is a selective and reversible inhibitor of the activity of ATM and thus can be used to transiently inhibit ATM kinase activity in cells (29). Previous work suggested that ATM has temporally distinct functions in cells exposed to IR. Transient inhibition of the kinase activity of ATM, from +15 to +75 min after IR, causes similar amounts of cell death as that caused by prolonged inhibition of ATM kinase activity, -45 min before through >16 hours after IR (29). Furthermore, 2 days after IR and transient inhibition of ATM kinase activity, cells in late S and G₂ phase, but not M phase, exhibited increased chromosome aberrations, indicating that the kinase activity of ATM is essential for DNA repair during the period +15 to +75 min after IR (29).

Here, we show that the ATM-dependent mechanisms that ensure cell survival and suppress chromosome aberrations within a few minutes to hours after IR are independent of the activity of DNA-PK and thus not likely mediated by NHEJ. In addition, neither the activation of nor the recovery from the IR-induced G₂-M cell cycle checkpoint was affected by inhibition of the kinase activity of ATM from +15 to +75 min after IR, indicating that 15 min of ATM kinase signaling was sufficient to induce this cell cycle checkpoint. We found that inhibition of the kinase activity of ATM from +15 to +75 min after IR abrogated IR-induced SCE, a process attributed to recombination-mediated repair. Either of two selective and reversible ATM inhibitors, KU55933 or KU60019, disrupted SCE caused by exposure of fibroblasts to camptothecin, a DNA-damaging agent. Because DNA damage-induced SCE occurred in A-T fibroblasts (lacking functional ATM protein), the ATM inhibitors had no effect on DNA damage-induced SCE in A-T fibroblasts, as expected. Thus, the consequences of short-term inhibition of the kinase activity of ATM and adaptation to loss of functional ATM protein are distinct, which may be of particular importance in a clinical setting where drugs are used to achieve short-term inhibition.

RESULTS

A brief period of ATM activity after IR is sufficient to trigger the G₂-M cell cycle checkpoint and subsequent transient inhibition of ATM does not affect recovery from this checkpoint

Because the reversible inhibition of ATM by KU55933 had only been shown by removal of the inhibitor before exposure of the fibroblasts to IR, we confirmed the reversibility of KU55933 inhibition of ATM activity induced by exposure of fibroblasts to IR. Fibroblasts were exposed to 2 Gy IR, treated with KU55933 from +15 to +75 min or from +15 to +90 min, and then ATM autophosphorylation was assayed at either +75 min or +90 min (Fig. 1, A and B). Fifteen minutes after removal of KU55933, we de-

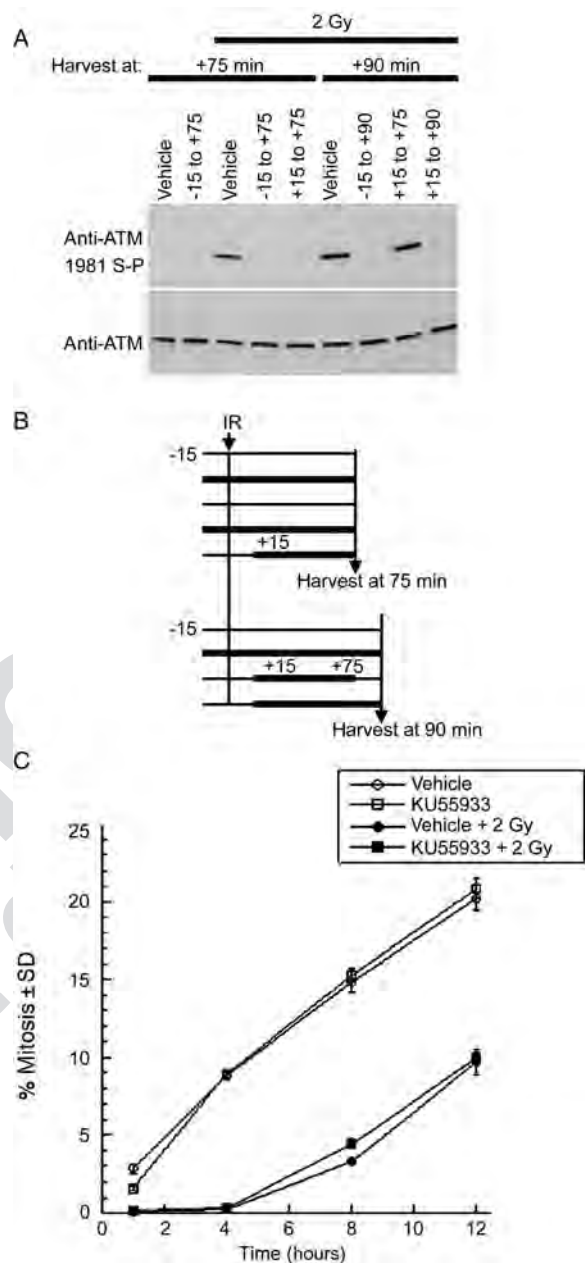


Fig. 1. Temporal dynamics of reversibility of inhibition of ATM. (A) IMR90 fibroblasts were treated with 10 μ M KU55933 from -15 to +90 min, +15 to +75 min, or +15 to +90 min after 2 Gy IR and harvested at +90 min. The kinase activity of ATM activity was restored when KU55933 was removed from +75 to +90 min after 2 Gy IR. (B) Diagram of the experimental paradigm for samples evaluated in (A). Thick bars indicate when KU55933 was present. (C) IMR90 fibroblasts were treated with KU55933 from +15 to +75 min after 2 Gy IR, KU55933 was removed, and nocodazole was added to collect fibroblasts that entered into mitosis. Fibroblasts were collected at +75 min, 4, 8, and 12 hours after IR for flow cytometric analysis of DNA content (% mitosis reflects 4N fibroblasts positive for phosphorylated histone H3 at +75 min). Recovery from the G₂-M checkpoint was not perturbed by addition of KU55933 from +15 to +75 min after 2 Gy IR. This experiment was performed in triplicate three times.

tected ATM autophosphorylation, indicating that the inhibition of IR-induced ATM activity was reversible.

Because transient ATM kinase inhibition from +15 to +75 min after exposure of cells to IR is sufficient to cause the accumulation of persistent chromosome aberrations in late S- and G₂-, but not M-phase, cells, we hypothesized that the ATM-dependent G₂-M cell cycle checkpoint may be induced within 15 min of exposure to 2 Gy IR. We observed that induction of the G₂-M cell cycle checkpoint occurred rapidly in IMR90 fibroblasts treated with either KU55933 or vehicle from +15 to +75 min after exposure to 2 Gy IR, as indicated by the reduction of 4N cells positive for phosphorylated histone H3 at +75 min (Fig. 1C). Furthermore, the recovery from the G₂-M arrest in IMR90 fibroblasts treated with KU55933 from +15 to +75 min was comparable to that of vehicle controls at 4, 8, and 12 hours after IR (Fig. 1C). Thus, 15 min of ATM activity is sufficient for the induction of the G₂-M cell cycle checkpoint after 2 Gy IR, and transient inhibition of the kinase activity of ATM from +15 to +75 min does not affect recovery from this cell cycle checkpoint.

The early phase of IR-induced ATM activity that ensures cell survival is independent of DNA-PK activity

Given that transient ATM kinase inhibition from +15 to +75 min after IR radiosensitizes cells and results in persistent chromosome aberrations in late S- and G₂-phase cells (29) and that we determined this was not due to defective checkpoint activation, we investigated the underlying mechanisms of chromosome stability and cellular radioprotection that require the kinase activity of ATM. To determine if ATM was stimulating DNA repair through NHEJ at this time, we exposed fibroblasts to the selective and reversible inhibitor of DNA-PK activity, NU7441 (30). We determined the reversibility of DNA-PK inhibition upon removal of 5 μM NU7441 from fibroblasts by examining DNA-PK autophosphorylation on Ser²⁰⁵⁶ in IMR90 human fibroblasts (31). In IMR90 fibroblasts exposed to 5 μM NU7441 for 30, 15, or 5 min before exposure to 5 Gy IR, as well as for 15 min after exposure to IR, IR-induced autophosphorylation of DNA-PK was inhibited (Fig. 2, A and C). In contrast, IR-induced autophosphorylation of DNA-PK was restored in fibroblasts in which NU7441 was removed less than 5 min before exposure to IR (Fig. 2, B and D). Because the fibroblasts were harvested 15 min after exposure to IR, the reversibility of DNA-PK inhibition upon removal of 5 μM NU7441 from IMR90 fibroblasts requires less than 15 min. The reversibility of DNA-PK inhibition by NU7441 in IMR90 fibroblasts is similar to the inhibition of the kinase activity of ATM by KU55933 (29); thus, NU7441 can be used to transiently inhibit DNA-PK activity in fibroblasts. We confirmed that 5 μM NU7441 did not inhibit the kinase activity of ATM activity and that 10 μM KU55933 did not inhibit the kinase activity of DNA-PK in fibroblasts exposed to IR (Fig. 2E).

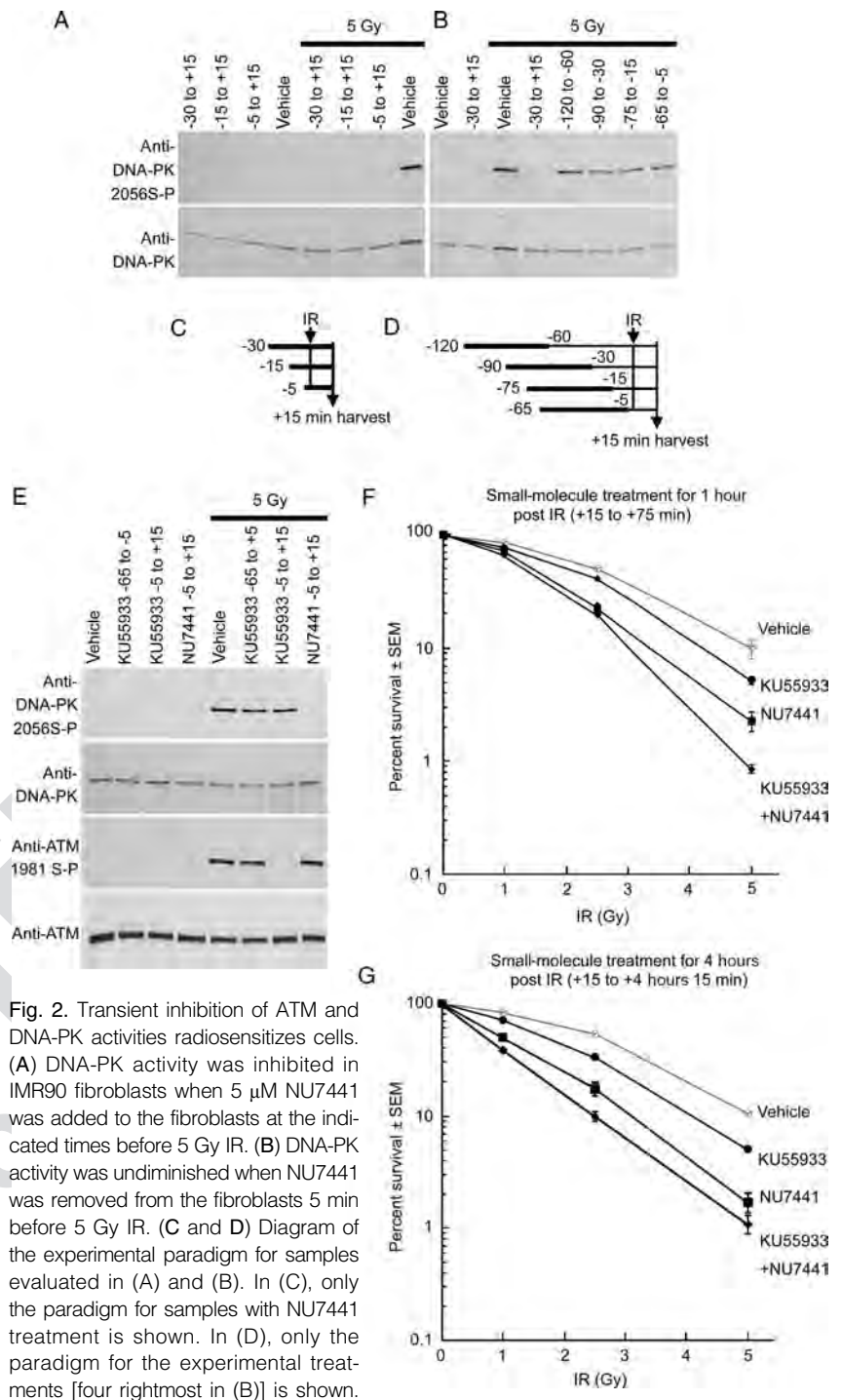


Fig. 2. Transient inhibition of ATM and DNA-PK activities radiosensitizes cells. (A) DNA-PK activity was inhibited in IMR90 fibroblasts when 5 μM NU7441 was added to the fibroblasts at the indicated times before 5 Gy IR. (B) DNA-PK activity was undiminished when NU7441 was removed from the fibroblasts 5 min before 5 Gy IR. (C and D) Diagram of the experimental paradigm for samples evaluated in (A) and (B). In (C), only the paradigm for samples with NU7441 treatment is shown. In (D), only the paradigm for the experimental treatments [four rightmost in (B)] is shown. Thick bars indicate when NU7441 was present. (E) The kinase activity of ATM was inhibited in IMR90 fibroblasts after irradiation when 10 μM KU55933 was added 5 min before the 5 Gy IR. The kinase activity of ATM was undiminished 15 min after irradiation when KU55933 was removed 5 min before 5 Gy IR. (F) Cell survival was assayed after 1 hour of inhibition of ATM or DNA-PK activities from +15 to +75 min after 5 Gy IR. Inhibition of DNA-PK had a greater effect on cell survival than did ATM inhibition at both 2.5 and 5 Gy. (G) Cell survival was assayed after 4 hours of inhibition of ATM or DNA-PK activities from +15 min to +4 hours 15 min after 5 Gy IR. DNA-PK inhibition caused greater radiosensitization than did ATM inhibition. Experiments shown in (F) and (G) were performed in triplicate three times.

To determine the effect that inhibition of these two kinases had on cell survival, we determined the clonogenic survival of H460 non-small cell lung carcinoma cells (p53 wild-type cells) at 10 days when the kinase activity of ATM or DNA-PK, or both, had been transiently inhibited for either 1 hour or 4 hours after exposure to IR. Transient inhibition of the kinase activity of either ATM or DNA-PK from +15 to +75 min after exposure to 1, 2.5, or 5 Gy IR resulted in increased cell death compared to that of vehicle-treated control cells, indicating radiosensitivity of the kinase-inhibited cells (Fig. 2F). Concurrent inhibition of both ATM and DNA-PK kinase activities resulted in greater cell death than occurred when each kinase was inhibited individually, with the greatest increase in cell death of the dually inhibited cells at the highest dose of IR. Inhibition of the kinase activity of ATM or DNA-PK activities from +15 to +75 min after exposure of cells to 5 Gy IR accounted for 53 and 85%, respectively, of the cell death that occurred in cells in which both kinases were inhibited; whereas in cells exposed to 2.5 Gy IR, individual kinase inhibition accounted for 28% (ATM) and 90% (DNA-PK) of the cell death that occurred in dually inhibited cells (Fig. 2F). We also inhibited the kinase activity of ATM or DNA-PK, or both, for 4 hours, from +15 min to +4 hours 15 min, after IR (Fig. 2G). Concurrent inhibition of both ATM and DNA-PK kinase activities resulted in a greater cell death than occurred when each kinase was inhibited individually. Inhibition of ATM or DNA-PK kinase activities from +15 min to +4 hours 15 min after 5 Gy IR accounted for 58 and 94%, respectively, of the radiosensitization seen after inhibition of both kinases; at 2.5 Gy IR it accounted for 47% (ATM) and 83% (DNA-PK). The results from this longer exposure to the drugs indicate that the differences in cell survival did not relate to differences in the half-lives of the two drugs, which would not be evident during a 4-hour inhibition. Because inhibition of ATM activity promoted IR-induced cell death even when DNA-PK was functional, the ATM kinase-dependent mechanism that contributes to cell survival from +15 min to +4 hours 15 min after exposure to IR is independent of DNA-PK-dependent NHEJ. Additionally, these data suggest that DNA-PK-dependent, ATM-independent NHEJ is the principal mechanism of cellular radioprotection from +15 min to +4 hours 15 min after exposure to IR.

The early phase of IR-induced ATM activity that prevents the accumulation of chromosome aberrations is independent of DNA-PK activity

Persistent chromosome aberrations accumulate in late S- and G₂-, but not M-phase cells when the kinase activity of ATM activity is inhibited from +15 to +75 min after exposure to 2 Gy IR (29). Here, we show that persistent chromosome aberrations accumulate in fibroblasts when DNA-PK kinase activity was inhibited from +15 to +75 min after exposure to IR. IMR90 fibroblasts were exposed to a dose titration of IR 48 hours before harvest with calyculin A, a serine-threonine phosphatase inhibitor that prematurely condenses chromatin and allows visualization of late S-, G₂-, and M-phase cells, as previously described (29). The number of chromosome aberrations per cell was then enumerated in 50 cells. Further, the amount of persistent chromosome aberrations increased with the dose of IR, showing a linear relationship to IR dose in fibroblasts in which either the kinase activity of DNA-PK (Fig. 3, A and B, and table S2) or ATM (Fig. 3, C and D, and table S1) was transiently inhibited from +15 to +75 min after exposure to IR.

The number of chromosome aberrations seen in late S- and G₂-, but not M-phase, fibroblasts when the activities of both ATM and DNA-PK were concurrently inhibited from +15 to +75 min after exposure to 2 Gy IR was approximately equal to the sum of the number of chromosome aberrations in IR-exposed fibroblasts in which each kinase was inhibited individually (Fig. 4A and table S3). IMR90 fibroblasts were exposed to 2 Gy

before harvest with either calyculin A or colcemid, a microtubule inhibitor that allows visualization of M-phase cells, as previously described (29). Because we observed an increase in chromosome aberrations in cells harvested in late S-, G₂-, and M-phase fibroblasts generated with calyculin A, but not in harvests of M-phase fibroblasts generated with colcemid, we conclude that the chromosome aberrations that accumulated when the kinase activity of DNA-PK was inhibited were in late S- and G₂-phase fibroblasts. We performed similar experiments in which the activity of the kinases separately or together was inhibited for 4 hours, from +15 min to +4 hours 15 min, after exposure to IR. With this longer inhibition of kinase activity, the number of chromosome aberrations induced by 2 Gy IR in late S- and G₂-phase fibroblasts when both ATM and DNA-PK activities were concurrently inhibited was greater than the sum of the number of chromosome aberrations that occurred in IR-exposed fibroblasts in which each kinase was inhibited individually (Fig. 4B and table S4). Because ATM kinase inhibition resulted in an accumulation of chromosome aberrations in the presence of the DNA-PK inhibitor, we conclude that an ATM-dependent mechanism

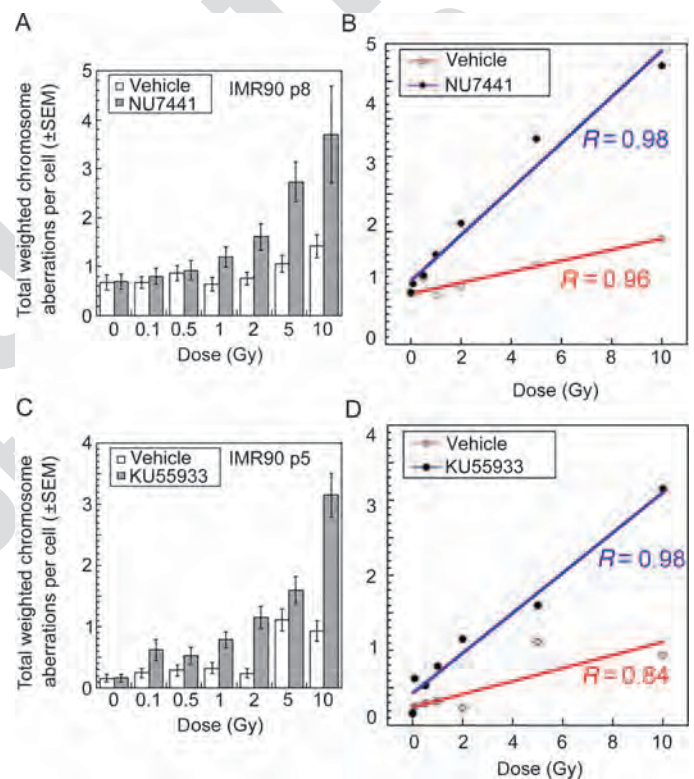


Fig. 3. Transient inhibition of either ATM or DNA-PK activities results in an IR dose-dependent and linear accumulation of persistent chromosome aberrations in late S-, G₂-, and M-phase fibroblasts. (A) IMR90 fibroblasts were treated with 5 μ M NU7441 from +15 to +75 min after 2 Gy IR and fibroblasts were harvested by applying calyculin A 48 hours after IR and analyzed for chromosome aberrations (table S2). (B) The DNA-PK-dependent mechanism of chromosome stability appears to increase linearly with IR dose. The linear correlation coefficients indicate a high degree of correlation. (C) IMR90 fibroblasts were treated with 10 μ M KU55933 from +15 to +75 min after 2 Gy IR and fibroblasts were isolated by applying calyculin A 48 hours after IR and analyzed for chromosome aberrations (table S1). (D) The ATM-dependent mechanism of chromosome stability appears to increase linearly with IR dose. The linear correlation coefficients indicate a high degree of correlation.

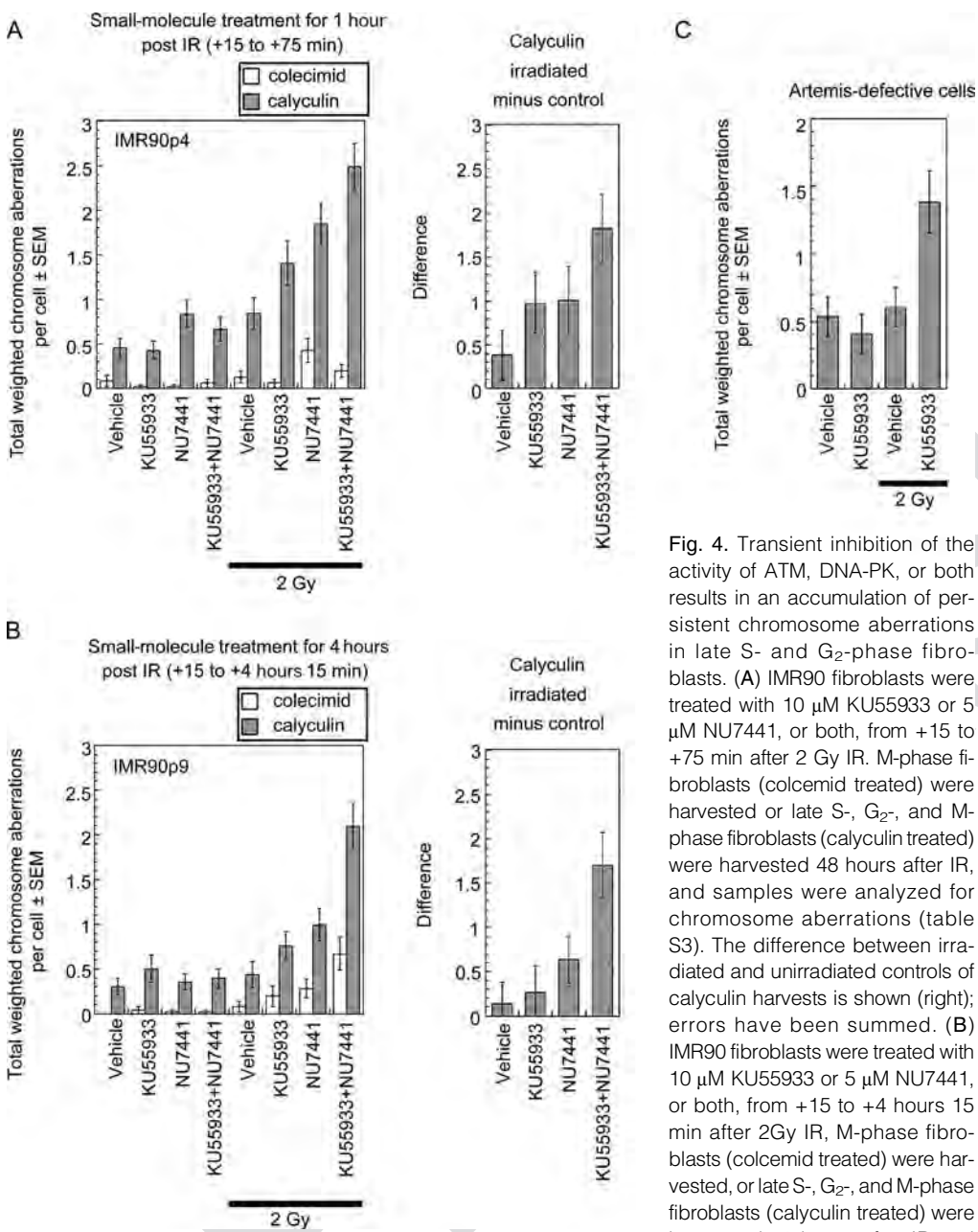


Fig. 4. Transient inhibition of the activity of ATM, DNA-PK, or both results in an accumulation of persistent chromosome aberrations in late S- and G₂-phase fibroblasts. (A) IMR90 fibroblasts were treated with 10 μM KU55933 or 5 μM NU7441, or both, from +15 to +75 min after 2 Gy IR. M-phase fibroblasts (colcemid treated) were harvested or late S-, G₂- and M-phase fibroblasts (calyculin treated) were harvested 48 hours after IR, and samples were analyzed for chromosome aberrations (table S3). The difference between irradiated and unirradiated controls of calyculin harvests is shown (right); errors have been summed. (B) IMR90 fibroblasts were treated with 10 μM KU55933 or 5 μM NU7441, or both, from +15 to +4 hours 15 min after 2Gy IR. M-phase fibroblasts (colcemid treated) were harvested, or late S-, G₂- and M-phase fibroblasts (calyculin treated) were harvested 48 hours after IR and analyzed for chromosome aberrations (table S4). The difference between irradiated and unirradiated controls of calyculin harvests is shown (right); errors have been summed. The experiments described in (A) and (B) were performed twice. (C) Artemis-defective fibroblasts were treated with 10 μM KU55933 from +15 to +75 min after 2Gy IR and late S-, G₂- and M-phase fibroblasts were isolated by applying calyculin A 48 hours after IR and analyzed for chromosome aberrations (table S5).

(23). To determine whether ATM was acting through an Artemis-dependent mechanism to limit persistent chromosomal instability caused by IR, we assessed the chromosome aberrations in CJ179 Artemis-deficient fibroblasts when the kinase activity of ATM was inhibited from +15 to +75 min after exposure to IR. The number of chromosome aberrations was increased under these conditions compared to vehicle-treated control CJ179 fibroblasts that were exposed to IR (Fig. 4C and table S5). Thus, the mechanism by which ATM prevents persistent chromosome instability after exposure to IR is independent of the endonuclease Artemis. We did not analyze DSBs in G₁-phase cells, where Artemis-mediated repair may be most important. Furthermore, previous work suggests that Artemis-mediated mechanism of DSB repair that is stimulated by ATM may not be required in S-phase cells to resolve DNA damage (28).

Transient inhibition of ATM activity after IR is sufficient to accumulate RPA34 foci

To investigate if, in cells exposed to IR, ATM acted through HR repair, we quantified nuclear foci positive for 53BP1 and γ-H2AX, two proteins that accumulate at DSBs (32–34), and foci positive for replication protein A (RPA), which indicate regions of single-stranded DNA (15). 200 fibroblasts were scored for each set of conditions. 53BP1 and γ-H2AX foci were increased 1, 4, and 12 hours after exposure of IMR90 fibroblasts to IR (Fig. 5A). Inhibition of ATM activity from +15 to +75 min after IR had no significant effect on either the incidence or the disappearance of 53BP1 and γ-H2AX foci, reflecting the occurrence of DSBs and their resolution. The numbers of 53BP1 and γ-H2AX foci were greatest at 1 hour after IR in both fibroblasts treated with or without KU55933. These data suggest that

that suppresses chromosomal instability in late S- and G₂-phase fibroblasts after IR is independent of DNA-PK-dependent NHEJ.

More evidence that NHEJ is not the primary mechanism for the early phase of ATM-mediated prevention of chromosomal instability after exposure of cells to IR came from analysis of fibroblasts deficient in Artemis, which is a component of the NHEJ machinery. Although ATM can stimulate the activity of Artemis, ATM-dependent Artemis activity is required for the resolution of only ~10% of DSBs that are repaired several hours after IR

there is no gross change in the number of DSBs or the kinetics of their repair, at this level of sensitivity, when the kinase activity of ATM is transiently inhibited from +15 to +75 min after exposure to IR.

In contrast to DSBs, we observed an increase in the percentage of fibroblasts positive for single-stranded DNA (RPA34 foci) at 12 hours after exposure to IR when the kinase activity of ATM was transiently inhibited from +15 to +75 min after exposure to IR (Fig. 5B). Using a comparison of means from unpaired data, we observed an increase (P = 0.08) in the per-

centage of fibroblasts positive for RPA34 foci, but not γ -53BP1 foci ($P = 0.41$) or H2AX foci ($P = 0.26$), 12 hours after exposure to IR when the kinase activity of ATM was transiently inhibited after exposure to IR. The accumulation and persistence of RPA34 foci in fibroblasts in which ATM was inhibited from +15 to +75 min after IR suggests that regions of single-stranded DNA are not being repaired efficiently, which could be a result of disrupted recombination-mediated repair.

Transient inhibition of ATM activity after IR abrogates IR-induced SCE

SCE is believed to be a recombination-mediated mechanism for the repair of stalled and collapsed DNA replication forks, which arise naturally during DNA replication or can occur if cells are irradiated in G₁ or S phase (35). SCE is normal in A-T cells (19–21). However, given that we found that the mechanism by which ATM ensures chromosomal stability in late S- and G₂-phase fibroblasts from +15 to +75 min after IR was independent of NHEJ, and that we determined that the G₂-M cell cycle checkpoint initiation and recovery occurred with kinetics in fibroblasts in which ATM was inhibited +15 to +75 min after IR that were identical to those in fibroblasts in which ATM was active, we compared the number of IR-induced SCEs in fibroblasts entering mitosis in the presence or absence of functional ATM. We examined GM09607 A-T fibroblasts, lacking ATM protein, and IMR90 fibroblasts, with functional ATM protein. We quantified the number of SCEs per cell from fibroblasts harvested after a 4-hour treatment with colcemid (from +16 to +20 hours), which was initiated 16 hours after IR, to trap cells in mitosis.

In unirradiated A-T fibroblasts, we observed ~12 SCEs per cell both in fibroblasts treated with or without the ATM inhibitor (Fig. 6A). Inhibition of ATM activity also did not change the number of SCEs (~17) in A-T fibroblasts 20 hours after exposure to 2 Gy IR. Thus, KU55933 does not appear to have “off-target” effects that disrupt SCE in A-T fibroblasts.

In unirradiated IMR90 fibroblasts, we observed ~6 SCEs per cell, irrespective of treatment with KU55933 or NU7441 (Fig. 6, B to D). This is concordant with expected spontaneous rates of SCE in normal fibroblasts (35). Although we expected the frequency of SCEs to increase in irradiated

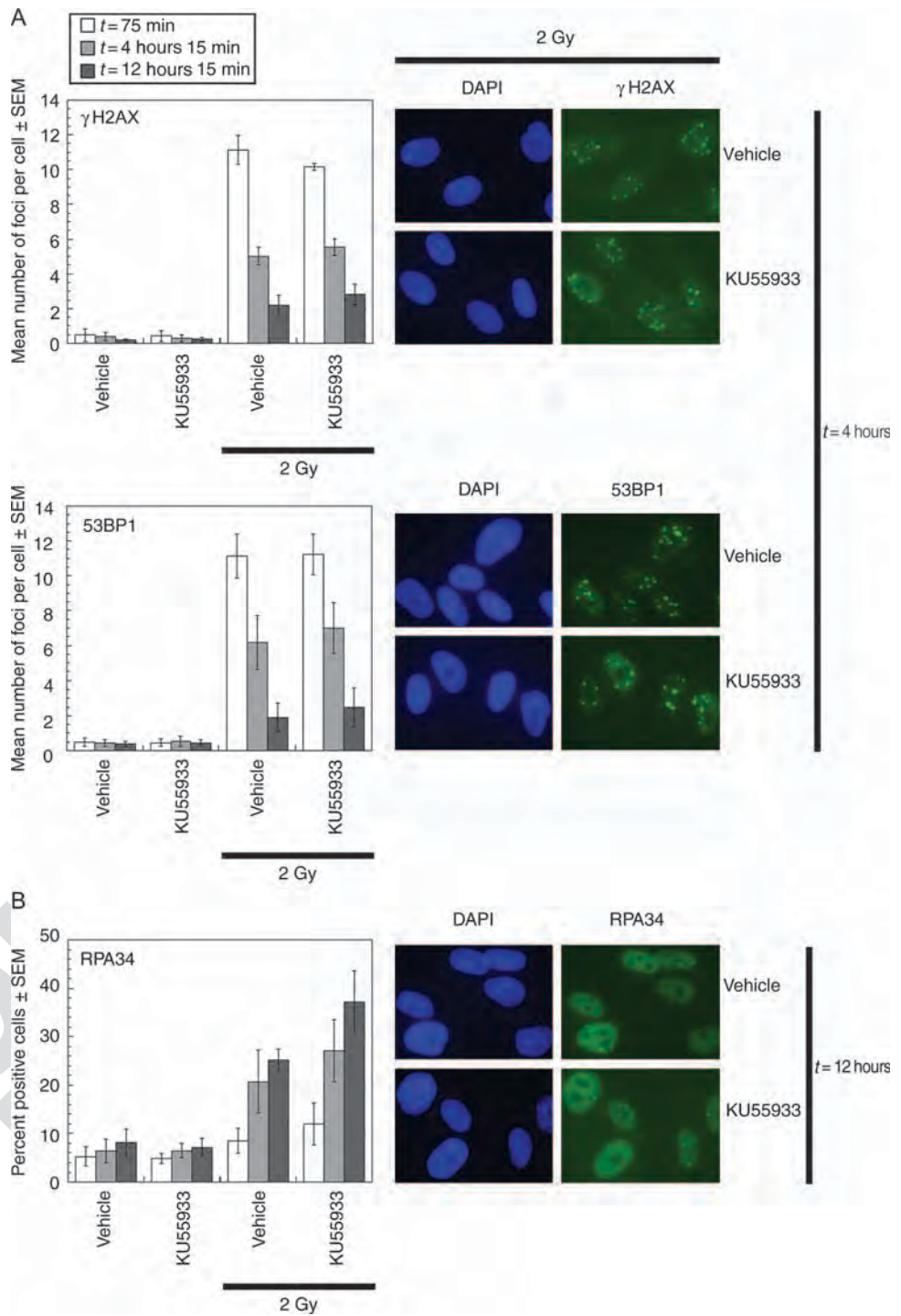


Fig. 5. Transient inhibition of the kinase activity of ATM affects the kinetics of DNA repair. Fibroblasts exposed to KU55933 were exposed from +15 to +75 min after 2 Gy IR and then fibroblasts were collected and analyzed at the indicated times. (A) The numbers of nuclear foci positive for 53BP1 or γ -H2AX foci were greatest at 1 hour after IR irrespective of treatment with KU55933. No difference in the appearance or resolution of either 53BP1 or γ -H2AX foci in cells treated or not treated with KU55933. Representative images at 4 hours after IR are presented at right. (B) A higher percentage of fibroblasts were positive for RPA34 foci at 12 hours after IR when ATM was inhibited from +15 to +75 min. Representative images at 12 hours after IR are presented at right. These experiments were performed three times.

IMR90 fibroblasts regardless of ATM kinase inhibition (as is the case in irradiated A-T fibroblasts), instead we found that IR-induced SCE was reduced (from 5 to 1 SCE per cell) in normal fibroblasts when ATM activity was transiently inhibited from +15 to +75 min (Fig. 6, B to D) or from +15 min to 4 hours 15 min (Fig. 6C) after IR. Because IR-induced SCE was maintained in A-T fibroblasts that lack ATM protein and the ATM inhibitors had no effect on IR-induced SCE in A-T fibroblasts, these data reveal that the cellular consequences of transient ATM inhibition and complete and prolonged loss of ATM protein are distinct.

In contrast to fibroblasts in which ATM was inhibited, the number of IR-induced SCEs was increased when DNA-PK activity was transiently inhibited for 1 hour after IR (Fig. 6B), suggesting that, in the absence of NHEJ, more DNA damage is resolved by SCE. The number of IR-induced SCEs was not changed when ATM and DNA-PK activities were concurrently inhibited for 1 hour after IR. One possible explanation for this observation is that an SCE mechanism that is independent of ATM functions at a subset of DSBs that persist when NHEJ is also inhibited. Because IR-induced SCE is intact in A-T fibroblasts, an ATM independent mechanism of SCE exists (Fig. 6A) (19–21).

We compared the number of IR-induced SCEs in fibroblasts entering mitosis in the presence or absence of ATM inhibition as soon after cell cycle checkpoint recovery as possible. Recovery from the G₂-M arrest in IMR90 fibroblasts treated with KU55933 from +15 to +75 min after IR is comparable to that of vehicle controls at 4, 8, and 12 hours after IR (Fig. 1C). Therefore, we used a 4-hour treatment (from +8 to +12 hours) with colcemid, initiated 8 hours after IR, to trap cells in mitosis. We found that the IR-induced increase in SCE at 12 hours after the insult was abrogated when the kinase activity of ATM activity was inhibited from +15 to +75 min, but not from -45 to +15 min after exposure to IR (Fig. 6D). This suggests that the IR-induced increase in SCE is not a consequence of mitotic recombination or a second round of DNA replication.

Transient inhibition of ATM disrupts camptothecin-induced SCE

IR-induced SCEs are believed to arise through the recombination-mediated restart of damaged replication forks in cells irradiated in G₁ phase (35–38). To determine whether the kinase activity of ATM was required for the repair of collapsed replication forks, we used the DNA topoisomerase 1 (Top1) inhibitor camptothecin. Top1 relaxes positive DNA supercoiling ahead of

replication forks and transcription complexes and relaxes negative supercoiling that occurs behind such complexes. To relax the DNA, Top1 transiently cleaves one strand of duplex DNA by the nucleophilic attack of its active site tyrosine on the DNA phosphodiester backbone to yield a 3' phosphotyrosyl bond (39, 40). The plant alkaloid camptothecin converts this short-lived, covalent Top1-DNA cleavage complex (Top1cc) into irreversible Top1-DNA cleavage complexes (41). Top1-linked DNA single-

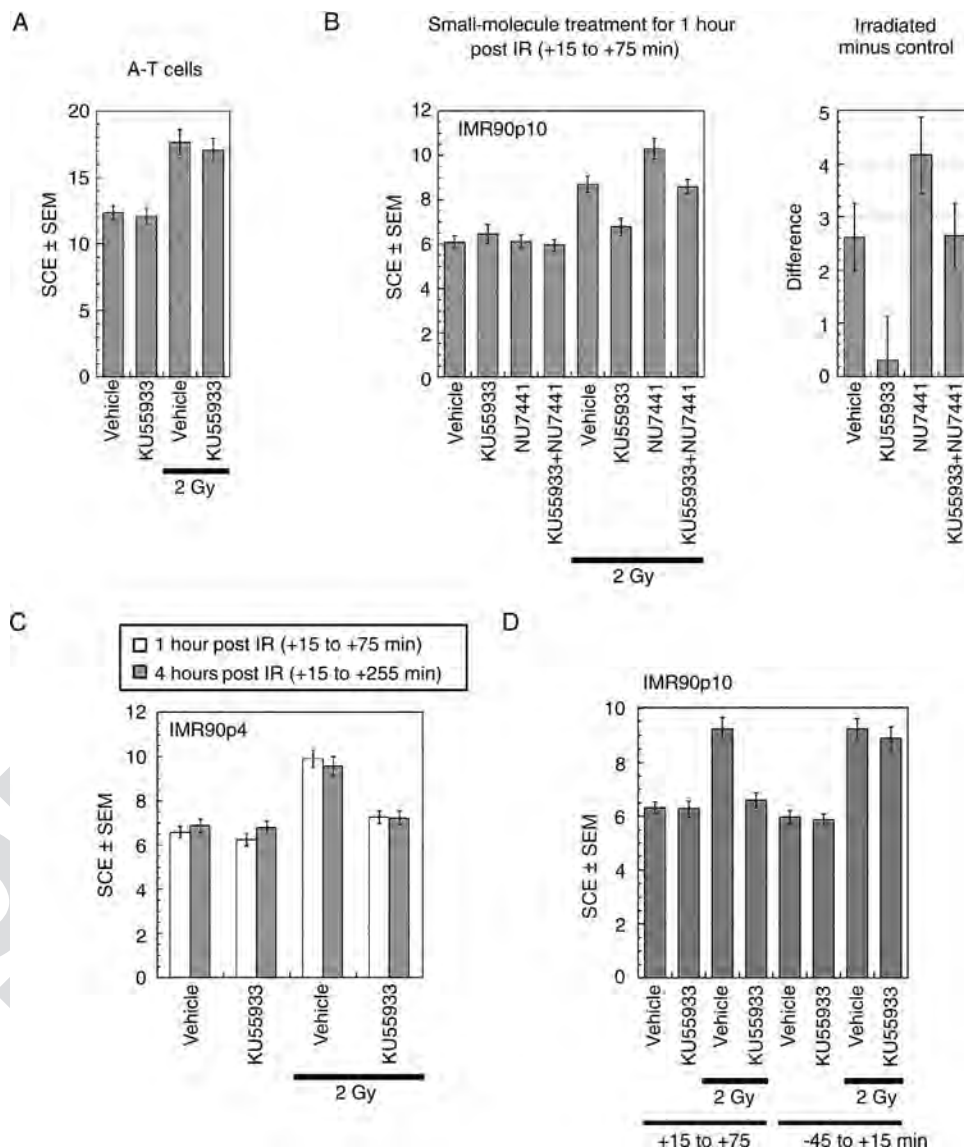


Fig. 6. Transient inhibition of ATM abrogates IR-induced SCE. (A) Treatment with 10 μ M KU55933 from +15 to +75 min after 2 Gy IR had no effect on IR-induced SCEs in GM09607 A-T fibroblasts at 20 hours. (B) Treatment with 10 μ M KU55933 from +15 to +75 min after 2 Gy IR abrogated IR-induced SCE in IMR90 fibroblasts at 20 hours. The difference between irradiated and unirradiated controls is shown (right); errors have been summed. (C) There is no difference in the number of SCEs when comparing 10 μ M KU55933 treatments from +15 to +75 min and +15 min to 4 hours 15 min after 2 Gy IR. (D) Treatment with 10 μ M KU55933 from +15 to +75 min after 2Gy IR abrogated IR-induced SCE in IMR90 fibroblasts at 12 hours. Treatment with 10 μ M KU55933 from -45 to +15 min after 2Gy IR had no effect on IR-induced SCE in IMR90 fibroblasts at 12 hours. For each experimental condition, the number of SCEs per cell was counted in 50 cells and each experiment was performed twice.

strand breaks can be subsequently transformed into DNA DSBs after collision with replication machineries in S phase (42).

We irradiated fibroblasts and then subjected them to the following treatments: camptothecin from 0 to +1 hour (to induce DNA single-stranded DNA breaks), KU55933 from 0 to +12 hours (to inhibit ATM), and colcemid from +8 to +12 hours (to trap cells in mitosis). Mitotic-arrested, camptothecin-treated fibroblasts had 18 SCEs per cell, whereas cells exposed to KU55933 had only 8 SCEs per cell (Fig. 7A).

KU60019 is another selective and reversible inhibitor of the kinase activity of ATM (43). We determined that 1 μ M KU60019 can also be used as a molecular switch to transiently inhibit ATM activity in cells and acted with similar kinetics to those of the ATM inhibitor KU55933 or the DNA-PK inhibitor NU7441 (fig. S1). Camptothecin-treated A-T fibroblasts had ~20 SCEs irrespective of treatment with 1 μ M KU60019, showing that this second ATM inhibitor had no off-target effect that disrupted camptothecin-induced SCE in A-T fibroblasts (Fig. 7B). Camptothecin-treated IMR90 fibroblasts had ~18 SCEs, whereas only 9 were seen in camptothecin-treated cells exposed to KU60019 (Fig. 7B). Thus, inhibition of ATM activity disrupts camptothecin-induced SCE. The occurrence of camptothecin-induced SCE in A-T fibroblasts suggests that these cells have adapted to the loss of ATM and can trigger SCE through an ATM-independent process.

DISCUSSION

We have previously shown that activation of the kinases ATM and CHK2 peaks within 15 min of exposure of cells to IR (6, 29). We have also shown that transient inhibition of ATM kinase activity from +15 to +75 min after IR results in an accumulation of persistent chromosome aberrations in late S- and G₂-phase cells and increased cell death (29). We show here that tran-

sient inhibition of DNA-PK activity from +15 to +75 min after cellular exposure to IR also causes an accumulation of persistent chromosome aberrations in late S- and G₂-phase fibroblasts and increased cell death. However, we found the ATM-dependent and DNA-PK-dependent mechanisms that ensure cell survival and suppress chromosome aberrations during this period after exposure of cells to IR are distinct. NHEJ acts through DNA-PK, and this was the principal mechanism mediating cellular radioprotection from +15 min to +4 hours 15 min after exposure to IR (Fig. 2).

We also show here that 15 min of ATM activity is sufficient to induce the G₂-M cell cycle checkpoint in response to IR and that neither the activation nor the recovery of this IR-induced cell cycle checkpoint was affected by inhibition of ATM activity from +15 to +75 min (Fig. 1). Thus, with selective and reversible ATM inhibitors, we identified two indispensable ATM-dependent mechanisms for resolving DNA damage in irradiated fibroblasts. In addition to its function immediately after exposure of fibroblasts to IR to initiate the G₂-M cell cycle checkpoint, we identified a function for sustained early ATM activity that is essential to ensure cell survival and prevent the accumulation of persistent chromosome aberrations in irradiated fibroblasts.

We provide evidence that this second function of sustained ATM activity is to promote IR-induced SCE. SCEs are believed to be a cytological manifestation of the repair of damaged or collapsed replication forks, which occur naturally during DNA replication or occur in cells irradiated in G₁ phase and to a lesser extent in S phase (35–38). We show here that the increase in SCE in irradiated fibroblasts was abrogated when the kinase activity of ATM was transiently inhibited from +15 to +75 min after exposure to IR (Fig. 6). Similarly, camptothecin-induced SCE was disrupted by ATM inhibition (Fig. 7). These data are surprising because DNA damage-induced SCE occurred in A-T fibroblasts (Figs. 6 and 7), suggesting that these fibroblasts have adapted to the loss of this function of ATM and can initiate SCE in response to DNA damage through an ATM-independent mechanism. One possible explanation for this difference in cellular responses may be that the inhibited ATM protein impedes a complementary mechanism of repair that functions to promote SCE in cells that have adapted to the absence of ATM protein.

The idea that the DNA damage-induced mechanism of SCE has been rewired after adaptation to loss of ATM such that ATM is no longer essential for SCE is consistent with reports of similar DNA damage-induced processes in other genetic deficiencies. For example, such rewiring has been observed for the DNA damage checkpoints that are predominantly p53- and CHK1-dependent in p53-proficient cells (44), but p53-deficient cells rely on CHK1 and the stress-activated kinase of the mitogen-activated protein kinase (MAPK) family p38 and its effector MAPK-activated protein kinase-2 (MK2) (27). Further, cells lacking both of the genes *Cdc25B* and *Cdc25C*, encoding the cell cycle-regulating phosphatases, have normal DNA damage responses, cell cycles, and regulation of the phosphatase CDC25A, despite the paradigm that entry into mitosis requires CDC25B and CDC25C (45). These, and our data, show that it can be misleading to predict a drug's effects solely on the basis of animal and cell models in which a protein's function is disrupted through genetic deletion. Studies with inhibitors or transient methods for disruption function are essential to determine the cellular consequences of short-term protein inhibition.

Our data with the ATM inhibitors are consistent with the persistence of IR-induced DNA lesions that occurred in G₁- or S-phase cells, despite normal induction and recovery from the G₂-M checkpoint. DSBs are processed in S- and G₂-phase cells through HR that requires end resection mediated by CtIP and the MRE11 complex (46). ATM promotes DSB end resection that generates the single-stranded DNA required for the activation of the kinase ATR and HR in S- and G₂-phase cells (18, 46–50). Although DSB end resection is delayed in A-T cells, DSB end resection

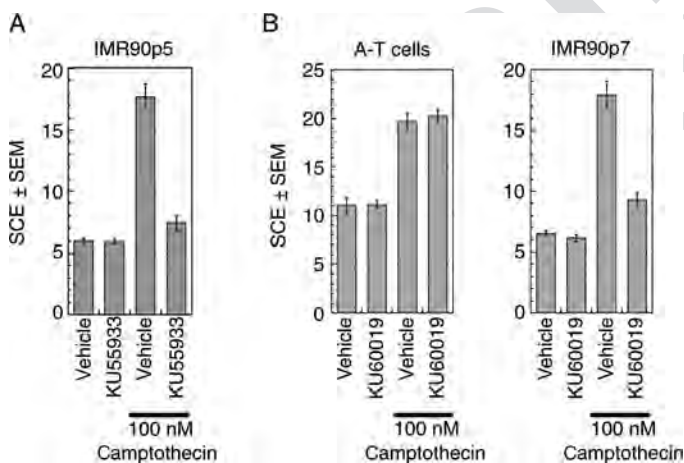


Fig. 7. ATM inhibition disrupts camptothecin-induced SCE. (A) Treatment of IMR90 fibroblasts with 10 μ M KU55933 and 100 nM camptothecin from 0 to 1 hour disrupts camptothecin-induced SCE at 12 hours. Cells were treated with camptothecin from 0 to 1 hour and KU55933 from 0 to 12 hours (B) Treatment with 1 μ M KU60019 and 100 nM camptothecin had no effect on camptothecin-induced SCEs in GM09607 A-T fibroblasts at 12 hours (left), but disrupts camptothecin-induced SCEs in IMR90 fibroblasts at 12 hours (right). Cells were treated with camptothecin from 0 to 1 hour and with 1 μ M KU60019 from 0 to 12 hours.

and ATR activation do occur (46–48). Our finding that, when ATM kinase is inhibited from +15 to +75 min after exposure to IR, RPA34 foci continued to accumulate 12 hours after exposure to IR suggests that regions of single-stranded DNA were not repaired efficiently (Fig. 5B). However, similar numbers of RPA foci were present at either 1 or 4 hours after irradiation in fibroblasts in which ATM was inhibited from +15 to +75 min or was not inhibited. This suggests that the initiation of DSB end resection is not impeded by short-term inhibition of ATM, but that repair of the resulting single-stranded DNA is.

Through analysis of the resolution γ -H2AX foci, ATM was found to be required for the repair of a subset of DSBs that are associated with heterochromatin in both NIH3T3 cells treated with KU55933 and A-T cells (51). The underlying mechanism was attributed to an ATM-dependent phosphorylation of KAP-1, an event that is critical for DSB repair of regions of compacted and inflexible chromatin (51). KAP-1 is a dedicated co-repressor for Krüppel-associated box (KRAB) zinc finger protein (ZFP) proteins. These studies were performed on asynchronous populations of cells and it is unclear whether this mechanism contributes to SCE in S-phase cells. The observation that DSB repair was impaired both in NIH3T3 cells treated with KU55933 and in A-T cells suggests that the ATM-dependent mechanism of SCE in S-phase cells that we have identified is not KAP-1-dependent. Nevertheless, it is possible that transient ATM inhibition impedes the repair of a subset of lesions that arise in heterochromatin during S phase.

ATM and Artemis are reported to promote the HR-mediated repair of ~15% of DSBs that arise in heterochromatin in G₂-phase cells (52). DSB repair was monitored through the resolution of γ -H2AX foci, and calyculin A was used to visualize late S-, G₂-, and M-phase chromosomes (52). In Artemis-defective CJ179 fibroblasts, ATM inhibition throughout the course of the experiment did not increase the frequency of chromosome breaks at 6 hours after 1 Gy IR (52). In contrast, we found that transient ATM inhibition after exposure to IR resulted in an increase in persistent chromosome aberrations in Artemis-defective CJ179 fibroblasts 48 hours after IR, indicating that ATM activity has Artemis-independent functions in DNA repair in either late S-, G₂-, or M-phase cells. The difference between the studies may be attributed to the different time points after irradiation at which the chromosomes were analyzed. In this recent study, the authors also reported that ATM protein knockdown in HeLa cells with small interfering RNA abrogated IR-induced SCE (52). These data differ from those presented here and previously reported in A-T fibroblasts that lack functional ATM protein (19–21). However, it is certainly possible that ATM protein is essential for IR-induced SCE in HeLa cells but not fibroblasts.

Our data add additional weight to previous findings that indicate that pharmacological ATM inhibition may have potential in the treatment of human cancers that experience replication stress as a consequence of somatic mutation. The FA pathway has an established role in the repair of stalled and collapsed DNA replication forks (53). The FA pathway is mutated in >10% of pancreatic cancers (54), and inhibition of ATM with KU55933 kills FA-deficient pancreatic tumor cell lines, but not isogenic corrected control cell lines, in the absence of exogenous DNA damage (26). These data are consistent with the hypothesis that ATM kinase has a direct role in a parallel pathway to FA for the repair of stalled and collapsed DNA replication forks and, therefore, is essential for the viability of pancreatic cancer cells that are defective in FA proteins. p53 is required for the activation of a G₁-S cell cycle checkpoint that prevents G₁-phase cells containing DNA damage from entering S phase (9). The p53 pathway is mutated in most tumor cells (55). Inhibition of ATM with KU55933 kills doxorubicin-treated p53-deficient lung tumor cell lines, lymphocytes, and MEFs (27, 28). Conversely, p53-proficient cell lines (and presumably “normal” cells and tissues) have increased resistance to doxorubicin when ATM is inhibited with KU55933 (27, 28). These data are consistent with

the hypothesis that ATM has a direct role in the repair of stalled and collapsed DNA replication forks in doxorubicin-treated p53-deficient cells, which are defective in the G₁-S cell cycle checkpoint and, therefore, is essential for the viability of doxorubicin-treated cancer cells that are defective in the p53 pathway. In contrast, doxorubicin-treated p53-proficient cells activate a normal G₁-S cell cycle checkpoint that prevents cells containing DNA damage from entering S phase, and inhibition of ATM may prevent doxorubicin-induced p53-dependent apoptosis (56).

In summary, we have shown that transient inhibition of the kinase activity of ATM disrupts DNA damage-induced SCE, indicating a function for ATM in the repair of stalled and collapsed DNA replication forks, in normal, but not A-T, fibroblasts. We show that the cellular consequences of short-term ATM kinase inhibition and adaptation to loss of ATM protein are different in S-phase cells.

MATERIALS AND METHODS

Cell lines, inhibitors, and irradiation

The transformed lung cell line NCI-H460 and the normal diploid fetal human lung fibroblast line IMR90 were obtained from the American Type Culture Collection. The A-T fibroblast line was obtained from the Coriell Institute for Medical Research. H460 cells were cultured in RPMI, and IMR90 and GM09607 were cultured in Dulbecco's modified Eagle's medium (DMEM); both media were supplemented with 10% fetal bovine serum (FBS). The Artemis-defective fibroblast line (CJ179-hTERT) was cultured in MEM supplemented with 15% FBS. KU55933 (57), KU60019 (43), and NU7441 (30) (KuDOS Pharmaceuticals) were reconstituted in dimethyl sulfoxide and used at final concentrations of 1, 10, and 5 μ M, respectively. Cells were γ -irradiated in a Shepherd Mark I Model 68 ¹³⁷Cs irradiator (J. L. Shepherd & Associates) at a dose rate of 77.0 roentgen (R)/min.

Antibodies

Rabbit polyclonal antibody against DNA-PK 2056S-P (Abcam), generic rabbit polyclonal antibody against DNA-PK (Cell Signaling), rabbit monoclonal antibody against ATM 1981S-P antisera (29) (Epitomics), and generic mouse monoclonal antibody against ATM antisera (Sigma) were used for immunoblotting. Mouse monoclonal antibody against 53BP1 and antibody against γ -H2AX antisera (Upstate) and rabbit polyclonal antibody against RPA antisera (NeoMarkers) were used for immunofluorescence. Whole-cell extracts were prepared in lysis buffer: 50 mM tris-HCl (pH 7.5), 150 mM NaCl, 50 mM NaF, 50 mM *N*-ethylmaleimide (NEM), 1% Tween-20, 0.5% NP-40, and 1 \times protease inhibitor cocktail (Roche Applied Science). Cleared cell extracts were resolved through 3 to 8% tris-acetate gels (Invitrogen).

G₂-M cell cycle checkpoint assays

IMR90 fibroblasts (500,000) were seeded in 60-mm dishes and exposed to 2 Gy IR 24 hours later. Fibroblasts were harvested at +75 min, +4, +8 hours, and +12 hours after IR. For the 4-, 8-, and 12-hour time points, medium containing KU55933 was removed at +75 min and replaced with pre-equilibrated medium containing nocodazole (100 ng/ml) to trap fibroblasts as they entered mitosis. Floating fibroblasts [obtained from medium or 1 \times phosphate-buffered saline (PBS) wash] and trypsinized fibroblasts were collected and fixed overnight at -20°C in ice-cold 70% ethanol-1 \times PBS. Fixed fibroblasts were permeabilized on ice for 8 min in 0.25% Triton X-100-PBS. Permeabilized fibroblasts were blocked in 1% bovine serum albumin-1 \times PBS for 1 hour, incubated with phosphohistone H3 (Ser¹⁰) Alexa Fluor 647-conjugated antibody (Cell Signaling) for 1 hour,

and counterstained with propidium iodide (Roche). At least 50,000 fibroblasts per condition were analyzed by flow cytometry (Dako CyAn) and data were analyzed with Summit software (Dako). All experiments were performed in triplicate and the experiment was performed three times.

Clonogenic survival assays

One thousand H460 cells were seeded in 60-mm dishes and irradiated after 4 hours, as previously described (29). Colonies were stained with 10% Giemsa-1× PBS solution after 10 days. A colony was defined as a cluster of ≥50 cells. All experiments were performed in triplicate.

Chromosome aberration analysis

Normal (IMR90) or Artemis-deficient (CJ179) fibroblasts were exposed to 2 Gy IR 48 hours before harvest in either 250 nM colcemid, a microtubule inhibitor that allows visualization of M-phase cells, or 50 nM calyculin A, a serine-threonine phosphatase inhibitor that prematurely condenses chromatin, allowing visualization of late S-, G₂-, and M-phase cells, as previously described (29). Chromosome spreads were harvested by conventional methods and solid-stained for 8 min in 4% Giemsa. Chromosome aberrations included chromosome breaks, chromatid gaps or breaks, quadriradials, triradials, giants, rings, minutes, dicentrics, fragments, and dots. Chromosome breaks, radials, giants, rings, and dicentrics were assigned twice the weight of the other aberrations for the purposes of analysis because they involve two chromatid events. The total weighted aberrations (TWAs) were determined per cell and the SEM was used as the estimate of error in the sample. In the dose titrations from 0.1 to 10 Gy, a linear fit was applied to the data, and the Pearson's *R* values were calculated. The experiments were performed two times.

Nuclear foci formation

IMR90 fibroblasts were cultured in single-well chamber slides (Nalge Nunc International) and exposed to 2 Gy IR. Fibroblasts were fixed with 2% paraformaldehyde (Sigma) for 30 min and permeabilized in 0.2% Triton X-100-1× PBS. Permeabilized fibroblasts were blocked in 5% donkey serum-1× PBS and incubated with antibody against γ-H2AX, antibody against 53BP1, or antibody against RPA34 for 1 hour. The primary antibody was detected with donkey antibody against mouse Alexa 488 (Molecular Probes) for 1 hour. Fibroblasts were counterstained with Vectashield mounting medium containing 4',6-diamidino-2-phenylindole (DAPI; Vector Laboratories) and analyzed with an epifluorescence microscope. A minimum of 200 fibroblasts was scored for each set of conditions. Results were reported as percent positive or the mean number of foci, and error was reported as SEM. The experiments were performed three times.

SCE analysis

Normal (IMR90) or A-T (GM09607) fibroblasts were exposed to one cycle substitution (20 hours) with 10 μM bromodeoxyuridine (BrdU) before exposure to 2 Gy IR. Fibroblasts were allowed to recover for an additional 20 hours after treatment before harvesting in 250 nM colcemid (Irvine Scientific) for 4 hours. Harvested fibroblasts were dropped onto slides by conventional methods and metaphase spreads were differentially stained for SCE analysis. In brief, slides were incubated in Hoechst 33258 for 10 min, immersed in 55°C 2× SSC while exposed to a black light at a distance of 10 cm for 15 min. Exposed slides were then stained in 4% Giemsa for 10 min. Non-centromeric SCEs were scored for 50 fibroblasts. The SEM was used as the estimate of error in the sample. The experiments were performed two times.

SUPPLEMENTARY MATERIALS

www.sciencesignaling.org/cgi/content/full/3/12/ra44/DC1

Fig. S1. KU60019 is another reversible inhibitor of ATM activity.

Table S1. Dose-dependent and KU55933-dependent increase in chromosome aberrations in IMR90 fibroblasts.

Table S2. Dose-dependent and NU7441-dependent increase in chromosome aberrations in IMR90 fibroblasts.

Table S3. Chromosome aberrations induced by 2 Gy IR in late-S and G₂-phase IMR90 fibroblasts (+15 to +75 min post-IR).

Table S4. Chromosome aberrations induced by 2 Gy IR in late-S and G₂-phase IMR90 cells (+15 to +225 min post-IR).

Table S5. Chromosome aberrations induced by 2 Gy IR Artemis-defective cells after inhibition of ATM for 1 hour.

REFERENCES AND NOTES

1. K. Savitsky, A. Bar-Shira, S. Gilad, G. Rotman, Y. Ziv, L. Vanagaite, D. A. Tagle, S. Smith, T. Uziel, S. Sfez, M. Ashkenazi, I. Pecker, M. Frydman, R. Harnik, S. R. Patanjali, A. Simmons, G. A. Clines, A. Sarti, R. A. Gatti, L. Chessa, O. Sanal, M. F. Lavin, N. G. Jaspers, A. M. Taylor, C. F. Arlett, T. Miki, S. M. Weissman, M. Lovett, F. S. Collins, Y. Shiloh, A single ataxia telangiectasia gene with a product similar to PI-3 kinase. *Science* **268**, 1749–1753 (1995).
2. S. Gilad, R. Khosravi, D. Shkedy, T. Uziel, Y. Ziv, K. Savitsky, G. Rotman, S. Smith, L. Chessa, T. J. Jorgensen, R. Harnik, M. Frydman, O. Sanal, S. Portnoi, Z. Goldwicz, N. G. Jaspers, R. A. Gatti, G. Lenoir, M. F. Lavin, K. Tatsumi, R. D. Wegner, Y. Shiloh, A. Bar-Shira, Predominance of null mutations in ataxia-telangiectasia. *Hum. Mol. Genet.* **5**, 433–439 (1996).
3. S. Banin, L. Moyal, S. Shieh, Y. Taya, C. W. Anderson, L. Chessa, N. I. Smorodinsky, C. Prives, Y. Reiss, Y. Shiloh, Y. Ziv, Enhanced phosphorylation of p53 by ATM in response to DNA damage. *Science* **281**, 1674–1677 (1998).
4. C. E. Canman, D. S. Lim, K. A. Cimprich, Y. Taya, K. Tamai, K. Sakaguchi, E. Appella, M. B. Kastan, J. D. Siliciano, Activation of the ATM kinase by ionizing radiation and phosphorylation of p53. *Science* **281**, 1677–1679 (1998).
5. P. J. McKinnon, ATM and ataxia telangiectasia. *EMBO Rep.* **5**, 772–776 (2004).
6. C. J. Bakkenist, M. B. Kastan, DNA damage activates ATM through intermolecular autophosphorylation and dimer dissociation. *Nature* **421**, 499–506 (2003).
7. S. Matsuoka, M. Huang, S. J. Elledge, Linkage of ATM to cell cycle regulation by the Chk2 protein kinase. *Science* **282**, 1893–1897 (1998).
8. R. B. Painter, B. R. Young, Radiosensitivity in ataxia-telangiectasia: A new explanation. *Proc. Natl. Acad. Sci. U.S.A.* **77**, 7315–7317 (1980).
9. M. B. Kastan, Q. Zhan, W. S. el-Deiry, F. Carrier, T. Jacks, W. V. Walsh, B. S. Plunkett, B. Vogelstein, A. J. Fornace Jr., A mammalian cell cycle checkpoint pathway utilizing p53 and GADD45 is defective in ataxia-telangiectasia. *Cell* **71**, 587–597 (1992).
10. F. Zampetti-Bosseler, D. Scott, Cell death, chromosome damage and mitotic delay in normal human, ataxia telangiectasia and retinoblastoma fibroblasts after x-irradiation. *Int. J. Radiat. Biol. Relat. Stud. Phys. Chem. Med.* **39**, 547–58 (1981).
11. T. A. Weinert, L. H. Hartwell, The RAD9 gene controls the cell cycle response to DNA damage in *Saccharomyces cerevisiae*. *Science* **241**, 317–322 (1988).
12. J. B. Little, H. Nagasawa, Effect of confluent holding on potentially lethal damage repair, cell cycle progression, and chromosomal aberrations in human normal and ataxia-telangiectasia fibroblasts. *Radiat. Res.* **101**, 81–93 (1985).
13. M. N. Comforth, J. S. Bedford, On the nature of a defect in cells from individuals with ataxia-telangiectasia. *Science* **227**, 1589–1591 (1985).
14. P. J. Smith, M. C. Paterson, Effect of aphidicolin on de novo DNA synthesis, DNA repair and cytotoxicity in γ-irradiated human fibroblasts. Implications for the enhanced radiosensitivity in ataxia telangiectasia. *Biochem. Biophys. Acta* **739**, 17–26 (1983).
15. J. San Filippo, P. Sung, H. Klein, Mechanism of eukaryotic homologous recombination. *Annu. Rev. Biochem.* **77**, 229–257 (2008).
16. C. Morrison, E. Sonoda, N. Takao, A. Shinohara, K. Yamamoto, S. Takeda, The controlling role of ATM in homologous recombinational repair of DNA damage. *EMBO J.* **19**, 463–471 (2000).
17. H. E. Bryant, T. Helleday, Inhibition of poly (ADP-ribose) polymerase activates ATM which is required for subsequent homologous recombination repair. *Nucleic Acids Res.* **34**, 1685–1691 (2006).
18. P. Huertas, F. Cortés-Ledesma, A. A. Sartori, A. Aguilera, S. P. Jackson, (2008) CDK targets Sae2 to control DNA-end resection and homologous recombination. *Nature* **455**, 689–692 (2008).
19. S. M. Galloway, H. J. Evans, Sister chromatid exchange in human chromosomes from normal individuals and patients with ataxia telangiectasia. *Cytogenet. Cell Genet.* **15**, 17–29 (1975).
20. C. R. Bartram, T. Koske-Westphal, E. Passarge, Chromatid exchanges in ataxia telangiectasia, Bloom syndrome, Werner syndrome, and xeroderma pigmentosum. *Ann. Hum. Genet.* **40**, 79–86 (1976).

21. S. M. Galloway, Ataxia telangiectasia: The effects of chemical mutagens and x-rays on sister chromatid exchanges in blood lymphocytes. *Mutat. Res.* **45**, 343–349 (1977).
22. J. A. Downs, S. P. Jackson, A means to a DNA end: The many roles of Ku. *Nat. Rev. Mol. Cell Biol.* **5**, 367–78 (2004).
23. E. Riballo, M. Kühne, N. Rief, A. Doherty, G. C. Smith, M. J. Recio, C. Reis, K. Dahm, A. Fricke, A. Krempler, A. R. Parker, S. P. Jackson, A. Gennery, P. A. Jeggo, M. A. Löbrich, pathway of double-strand break rejoining dependent upon ATM, Artemis, and proteins locating to γ -H2AX foci. *Mol. Cell Biol.* **16**, 715–724 (2004).
24. S. Matsuoka, B. A. Ballif, A. Smogorzewska, E. R. McDonald III, K. E. Hurov, J. Luo, C. E. Bakalarski, Z. Zhao, N. Solimini, Y. Lerenthal, Y. Shiloh, S. P. Gygi, S. J. Elledge, ATM and ATR substrate analysis reveals extensive protein networks responsive to DNA damage. *Science* **316**, 1160–1166 (2007).
25. J. V. Olsen, M. Vermeulen, A. Santamaria, C. Kumar, M. L. Miller, L. J. Jensen, F. Gnäd, J. Cox, T. S. Jensen, E. A. Nigg, S. Brunak, M. Mann, Quantitative phosphoproteomics reveals widespread full phosphorylation site occupancy during mitosis. *Sci. Signal.* **3**, ra3 (2010).
26. R. D. Kennedy, C. C. Chen, P. Stuckert, E. M. Archila, M. A. De la Vega, L. A. Moreau, A. Shimamura, A. D. D'Andrea, Fanconi anemia pathway-deficient tumor cells are hypersensitive to inhibition of ataxia telangiectasia mutated. *J. Clin. Invest.* **117**, 1440–1449 (2007).
27. H. C. Reinhardt, A. S. Aslanian, J. A. Lees, M. B. Yaffe, p53-deficient cells rely on ATM- and ATR-mediated checkpoint signaling through the p38MAPK/MK2 pathway for survival after DNA damage. *Cancer Cell* **11**, 175–189 (2007).
28. H. Jiang, H. C. Reinhardt, J. Bartkova, J. Tommiska, C. Blomqvist, H. Nevanlinna, J. Bartek, M. B. Yaffe, M. T. Hemann, The combined status of ATM and p53 link tumor development with therapeutic response. *Genes Dev.* **23**, 1895–1909 (2009).
29. J. S. White, S. Choi, C. J. Bakkenist, Irreversible chromosome damage accumulates rapidly in the absence of ATM kinase activity. *Cell Cycle* **7**, 1277–1284 (2008).
30. J. J. Leahy, B. T. Golding, R. J. Griffin, I. R. Hardcastle, C. Richardson, L. Rigoreau, G. C. Smith, Identification of a highly potent and selective DNA-dependent protein kinase (DNA-PK) inhibitor (NU7441) by screening of chromenone libraries. *Bioorg. Med. Chem. Lett.* **14**, 6083–6087 (2004).
31. B. P. Chen, D. W. Chan, J. Kobayashi, S. Burma, A. Asaithamby, K. Morotomi-Yano, E. Botvinick, J. Qin, D. J. Chen, Cell cycle dependence of DNA-dependent protein kinase phosphorylation in response to DNA double strand breaks. *J. Biol. Chem.* **280**, 14709–14715 (2005).
32. L. B. Schultz, N. H. Chehab, A. Malikzay, T. D. Halazonetis, p53 binding protein 1 (53BP1) is an early participant in the cellular response to DNA double-strand breaks. *J. Cell Biol.* **151**, 1381–1390 (2000).
33. E. P. Rogakou, D. R. Pilch, A. H. Orr, V. S. Ivanova, W. M. Bonner, DNA double-stranded breaks induce histone H2AX phosphorylation on serine 139. *J. Biol. Chem.* **273**, 5858–5868 (1998).
34. W. M. Bonner, C. E. Redon, J. S. Dickey, A. J. Nakamura, O. A. Sedelnikova, S. Solier, Y. Pommier, γ H2AX and cancer. *Nat. Rev. Cancer* **12**, 957–967 (2008).
35. D. M. Wilson III, L. H. Thompson, Molecular mechanisms of sister-chromatid exchange. *Mutat. Res.* **616**, 11–23 (2007).
36. R. B. Painter, A replication model for sister-chromatid exchange. *Mutat. Res.* **70**, 337–341 (1980).
37. J. E. Cleaver, Correlations between sister chromatid exchange frequencies and replication sizes. *Expl. Cell Res.* **136**, 27–30 (1981).
38. I. Schubert, Sister chromatid exchanges and chromatid aberrations: A comparison. *Biol. Zentbl.* **109**, 7–18 (1990).
39. J. J. Champoux, DNA topoisomerases: Structure, function, and mechanism. *Annu. Rev. Biochem.* **70**, 369–413 (2001).
40. J. C. Wang, Cellular roles of DNA topoisomerases: A molecular perspective. *Nat. Rev. Mol. Cell Biol.* **13**, 430–440 (2002).
41. Y. H. Hsiang, R. Hertzberg, S. Hecht, L. F. Liu, Camptothecin induces protein-linked DNA breaks via mammalian DNA topoisomerase I. *J. Biol. Chem.* **260**, 14873–14878 (1985).
42. L. F. Liu, S. D. Desai, T. K. Li, Y. Mao, M. Sun, S. P. Sim, Mechanism of action of camptothecin. *Ann. N. Y. Acad. Sci.* **922**, 1–10 (2000).
43. S. E. Golding, E. Rosenberg, N. Valerie, I. Hussaini, M. Frigerio, X. F. Cockcroft, W. Y. Chong, M. Hummerson, L. Rigoreau, K. A. Menear, M. J. O'Connor, L. F. Povirk, T. van Meter, K. Valerie, Improved ATM kinase inhibitor KU-60019 radiosensitizes glioma cells, compromises insulin, AKT and ERK prosurvival signaling, and inhibits migration and invasion. *Mol. Cancer Ther.* **8**, 2894–2902 (2009).
44. M. H. Lam, Q. Liu, S. J. Elledge, J. M. Rosen, Chk1 is haploinsufficient for multiple functions critical to tumor suppression. *Cancer Cell* **6**, 45–59 (2004).
45. A. M. Ferguson, L. S. White, P. J. Donovan, H. Piwnicka-Worms, Normal cell cycle and checkpoint responses in mice and cells lacking Cdc25B and Cdc25C protein phosphatases. *Mol. Cell Biol.* **25**, 2853–2860 (2005).
46. A. A. Sartori, C. Lukas, J. Coates, M. Mistrik, S. Fu, J. Bartek, R. Baer, J. Lukas, S. P. Jackson, Human CtIP promotes DNA end resection. *Nature* **450**, 509–514 (2007).
47. A. Jazayeri, J. Falck, C. Lukas, J. Bartek, G. C. Smith, J. Lukas, S. P. Jackson, ATM- and cell cycle-dependent regulation of ATR in response to DNA double-strand breaks. *Nat. Cell Biol.* **8**, 37–45 (2006).
48. J. S. Myers, D. Cortez, Rapid activation of ATR by ionizing radiation requires ATM and Mre11. *J. Biol. Chem.* **281**, 9346–9350 (2006).
49. G. E. Dodson, R. S. Tibbetts, DNA replication stress-induced phosphorylation of cyclic AMP response element-binding protein mediated by ATM. *J. Biol. Chem.* **281**, 1692–1697 (2006).
50. M. Cuadrado, B. Martinez-Pastor, M. Murga, L. I. Toledo, P. Gutierrez-Martinez, E. Lopez, O. Fernandez-Capetillo, ATM regulates ATR chromatin loading in response to DNA double-strand breaks. *J. Exp. Med.* **203**, 297–303 (2006).
51. A. A. Goodarzi, A. T. Noon, D. Deckbar, Y. Ziv, Y. Shiloh, M. Löbrich, P. A. Jeggo, ATM signaling facilitates repair of DNA double-strand breaks associated with heterochromatin. *Mol. Cell* **31**, 167–177 (2008).
52. A. Beucher, J. Birraux, L. Tchouandong, O. Barton, A. Shibata, S. Conrad, A. A. Goodarzi, A. Krempler, P. A. Jeggo, M. Löbrich, ATM and Artemis promote homologous recombination of radiation-induced DNA double-strand breaks in G2. *EMBO J.* **28**, 3413–3427 (2009).
53. G. L. Moldovan, A. D. D'Andrea, How the Fanconi anemia pathway guards the genome. *Annu. Rev. Genet.* **43**, 223–249 (2009).
54. M. S. van der Heijden, J. R. Brody, E. Gallmeier, S. C. Cunningham, D. A. Dezentje, D. Shen, R. H. Hruban, S. E. Kern, Functional defects in the Fanconi anemia pathway in pancreatic cancer cells. *Am. J. Pathol.* **165**, 651–657 (2004).
55. B. Vogelstein, D. Lane, A. J. Levine, Surfing the p53 network. *Nature* **408**, 307–10 (2000).
56. K. H. Vousden, X. Lu, Live or let die: The cell's response to p53. *Nat. Rev. Cancer* **2**, 594–604 (2002).
57. I. Hickson, Y. Zhao, C. J. Richardson, S. J. Green, N. M. Martin, A. I. Orr, P. M. Reaper, S. P. Jackson, N. J. Curtin, G. C. Smith, Identification and characterization of a novel and specific inhibitor of the ataxia-telangiectasia mutated kinase ATM. *Cancer Res.* **64**, 9152–9159 (2004).
58. **Acknowledgments:** We thank G. C. Smith, M. O'Connor, and S. P. Jackson for providing the ATM and DNA-PK kinase inhibitors, and P. Jeggo for providing the Artemis-deficient cells. We thank L. H. Thompson for helpful discussions and J. S. Greenberger for critically reviewing the manuscript. **Funding:** This work was supported by the Frieda G. and Saul F. Shapira BRCA Cancer Research Program (David C. Whitcomb), the Lung Cancer Research Foundation (C.J.B.), the Lung Cancer Specialized Program of Research Excellence (SPORE) grant P50 CA090440 (Jill Siegfried), the Breast Cancer Research Foundation (Nancy E. Davidson), and start-up funds from the Department of Radiation Oncology (C.J.B.). S.C. was supported by Predoctoral Training in Pharmacological Sciences Grant T32 GM008424 (Donald B. DeFranco). **Author contributions:** J.S.W. performed the chromosome, foci, and SCE analyses. S.C. performed the G₂-M cell cycle checkpoint analyses. C.J.B. performed the immunoblotting. J.S.W., S.C., and C.J.B. designed experiments, analyzed the data, and wrote the manuscript. **Competing interests:** None declared.

Submitted 24 November 2009

Accepted 13 May 2010

Final Publication 1 June 2010

10.1126/scisignal.2000758

Citation: J. S. White, S. Choi, C. J. Bakkenist, Transient ATM kinase inhibition disrupts DNA damage-induced sister chromatid exchange. *Sci. Signal.* **3**, ra44 (2010).